Detergent-Induced Reversible Denaturation of the Photosystem II Reaction Center: Implications for Pigment–Protein Interactions†

Guillermo Montoya,‡,§ Rafael Cases,‖ Rosalía Rodríguez,⊥ María Aured,‡ and Rafael Picorel*,‡

Estación Experimental de Aula Dei, CSIC, Apartado 202, 50080-Zaragoza, Spain, Instituto de Ciencia de Materiales de Aragón, CSIC–Universidad de Zaragoza, Plaza San Francisco s/n, 50009-Zaragoza, Spain, and Departamento de Bioquímica y Biología Molecular, Facultad de Químicas, Universidad Complutense, Madrid, Spain

Received June 23, 1994®

ABSTRACT: Incubation of the D1–D2–cytochrome *b*559 complex with Triton X-100 modified the protein secondary structure, caused significant spectral modifications, and reduced the formation of light-induced spin-polarized triplet electron paramagnetic resonance (EPR) signal. After 24 h of incubation, the absorption spectrum shifted from 675.5 to 671.5 nm and the fluorescence spectrum shifted from 682 to 672 nm. These shifts were accompanied by an increase in the chlorophyll fluorescence yield and by decreases in the intensity of the circular dichroism in the red region and the secondary electron transport activity. The intensity of the light-induced triplet EPR signal was also markedly reduced in the same experimental conditions. Substitution of dodecyl β-maltoside for Triton X-100 reversed all the above-mentioned parameters to the values exhibited by the native D1–D2–Cyt *b*559 complex, including the characteristic triplet EPR signal. We concluded that all observed changes were due to the destruction of P680 with Triton X-100 and to the reestablishment of P680 in the presence of dodecyl β-maltoside. The easier but certainly not the only possible explanation to all these phenomena is to consider a dimeric structure for P680, at least in its ground state, where interactions take place within the two dimeric chromophores and with the apoprotein. Such a dimeric structure would be very sensitive to small modifications of the P680 domain, which convert the dimer absorbing at 680 into two chlorophyll monomers absorbing near 670 nm. The dodecyl β-maltoside reestablished the structure of the native P680 domain.

The photosystem II reaction center (PSII RC)[1] is a typical membrane protein which catalyzes the first steps in the conversion of light into chemical energy, where electrons, protons, and molecular oxygen are produced during the process. PSII RC consists of several polypeptides, D1, D2, the α- and β-chains of the cytochrome (Cyt) *b*559 (Nanba & Satoh, 1987; Barber et al., 1987; Braun et al., 1990), and the *psbI* gene product (Ikeuchi & Inoue, 1988), and cofactors such as chlorophylls (Chl) *a*, pheophytins (Pheo) *a*, plastoquinones, β-carotenes, Fe, and Mn. However, the plastoquinones and the metal atoms are lost during the RC isolation process. In certain RC isolation procedures, some of the pigments can also be lost (Montoya et al., 1991, 1993).

A high primary structure homology has been revealed between the L–M heterodimer of the purple bacterial RC and the D1–D2 heterodimer of the PSII RC. This homology is higher in the primary donor and acceptor domains of the RCs (Youvan et al., 1984; Trebst, 1986; Michel & Deisenhofer, 1988; Diner et al., 1991). Computer models of PSII RC have also shown a pseudo-*C*2 symmetry axis creating two possible electron transfer pathways within the D1–D2 heterodimer, as in the case of the L–M of the purple bacterial RC. However, charge separation occurs exclusively along one branch under physiological conditions in bacteria (Budil et al., 1987; Kirmaier & Holten, 1987) and plants (Moënne-Loccoz et al., 1989).

The structure of the primary donor of PSII RC (P680) is currently a subject of debate. Some experiments seem to indicate that the P680 is made of a pair of interacting Chl (Braun et al., 1990; van Kan et al., 1990; Durrant et al., 1992), but others suggest that it behaves as a monomer (van Mieghem et al., 1991; van der Vos et al., 1992). The domain where the special pair is located plays an important role because this is where the first photochemical events, leading to the charge separation, occur. This protein domain seems particulalry unstable. For instance, incubation of the D1–D2–Cyt *b*559 complex with the nonionic detergent Triton X-100 (TX-100) modified the absorption spectra, causing a blue shift of the main red band and a parallel loss of the photochemical activity (Seibert et al., 1988; Chapman et al., 1988; McTavish et al., 1989; Braun et al., 1990; Tang et al., 1991). However, the complex was rather stable in the presence of the nonionic detergent dodecyl β-maltoside (DM) (Seibert et al., 1988; Chapman et al., 1988; McTavish et al., 1989).

In the present study we have partially denatured the D1–D2–Cyt *b*559 complex under controlled conditions with the detergent TX-100, resulting in significant changes of the spectroscopic properties and in a loss of the light-induced spin-polarized triplet EPR signal and the secondary electron transport activity. The modified complex regained its native secondary structure, spectral properties, and photochemical

† We acknowledge the financial support of the Dirección General de Ciencia y Tecnología (Grant PB 92-0125) of Spain. G.M. is grateful to the Diputación General de Aragón (DGA-CONAI) for financial support. M.A. is the recipient of a fellowship from the Ministry of Education and Science of Spain.

* Corresponding author.

‡ Estación Experimental de Aula Dei, CSIC.

§ Present address: European Molecular Biology Laboratory, Meyerhofstrasse 1, Postfach 10.2209, 69012 Heidelberg, Germany.

‖ Istituto de Ciencia de Materiales de Aragón, CSIC–Universidad de Zaragoza.

⊥ Universidad Complutense.

® Abstract published in *Advance ACS Abstracts,* September 1, 1994.

[1] Abbreviations: Chl, chlorophyll; CD, circular dichroism; cmc, critical micelle concentration; Cyt, cytochrome; DM, dodecyl β-maltoside; EPR, electron paramagnetic resonance; P680, primary electron donor of the photosystem II; Pheo, pheophytin; PSII, photosystem II; RC, reaction center; SiMo, silicomolybdate; TX-100, Triton X-100.

0006-2960/94/0433-11798$04.50/0 © 1994 American Chemical Society

activities after exchanging the "harsh" detergent TX-100 with DM, a "milder" detergent. Some considerations on the P680 structure are also presented.

MATERIALS AND METHODS

Reaction Center Isolation, Denaturation, and Detergent Exchange. The D1–D2–Cyt *b*559 complex was isolated from PSII membranes of sugar beet (*Beta vulgaris* L. cv Monohill). Highly active PSII membranes were purified according to Berthold et al. (1981), and the PSII RC was isolated as in Nanba and Satoh (1987) with some modifications (Montoya et al., 1991). The D1–D2–Cyt *b*559 complex obtained in this way maintained the same pigment stoichiometry as other equivalent preparations, i.e., 6 Chl, 2 β-carotene, and 1 Cyt *b*559 per 2 Pheo (Kobayashi et al., 1990; Gounaris et al., 1990; Montoya et al., 1991). After isolation, the complex was subjected to partial denaturation, in a buffer of 50 mM Tris-HCl, pH 7.2, containing 0.05% TX-100, at 4 °C in the dark. Spectra were recorded at different incubation times to monitor the denaturation process.

When the lower energy band of the D1–D2–Cyt *b*559 complex showed a maximum at 671.5 nm, the sample was subjected to detergent exchange using a small (1.5 × 3 cm) DEAE-Fractogel TSK 650s (Merck) column previously equilibrated with 50 mM Tris-HCl, pH 7.2. A sample corresponding to about 40 μg of Chl [determined using an ϵ = 74 $mM^{-1}\cdot cm^{-1}$ in the red band; see Dekker et al. (1989)] was loaded onto the column, which was washed initially with 100–150 mL of the equilibration buffer containing 2 mM DM, and then the complex was eluted with 150 mM NaCl in 50 mM Tris-HCl, pH 7.2, with 2 mM DM. The D1–D2–Cyt *b*559 complex was desalted by dialysis against 50 mM Tris-HCl, pH 7.2, for 1 h. When necessary, the sample was concentrated using an Amicon Ultrafiltration Cell equipped with PM-30 membranes.

The detergent was also exchanged by centrifuging the sample, previously diluted 7-fold in 50 mM Tris-HCl, pH 7.2, at 309000*g* for 3 h (McTavish et al., 1989). Then the resulting pellet was resuspended in the same buffer with 2 mM DM.

Optical Spectroscopy. Absorption spectra were recorded at 4 °C with a Shimadzu UVPC-2101 spectrophotometer using 1-cm path length cuvettes. Second derivatives of the spectra were calculated using the software of the spectrophotometer.

Fluorescence spectra of Chl were obtained in a Kontron SFM-25 spectrofluorometer at 4 °C with excitation at 430 nm. The detection was made with an exit slit of 1 nm. Tryptophan fluorescence spectra of the D1–D2–Cyt *b*559 complex were obtained with a Hitachi F-4500 spectrofluorometer using excitation and emission slits of 1 and 2.5 nm, respectively. The RC concentration was normalized by equalizing the absorption at 0.1 unit in the main red band. Samples were excited at 296 nm in order to avoid interference from TX-100, and the spectra were recorded in the 310–380-nm spectral range at 4 °C.

Circular dichroism was measured at 4 °C in a Jobin-Yvon Mark III dichrograph fitted with a 250-W xenon lamp. The spectra were recorded at 0.2 nm/s scanning speed using 1-cm path length cuvettes. Mean residue weight ellipticities were calculated assuming a value of 111 as the average molecular weight per amino acid residue and expressed in terms of θ (degrees·centimeter^2·decimole^{-1}).

Electron Paramagnetic Resonance Spectroscopy. EPR measurements were carried out with a Varian E-112 spectrometer working in the X-band at 4.5 K using a continuous-flow helium cryostat (Model ESR-900, Oxford Instruments).

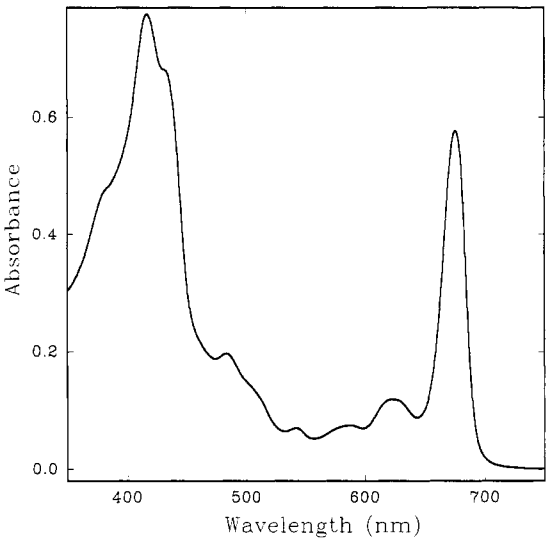

FIGURE 1: Electronic absorption spectrum of the D1–D2–Cyt *b*559 complex preparation from sugar beet in 50 mM Tris-HCl buffer, pH 7.2, with 0.05% TX-100. The spectrum were recorded immediately after the complex eluted from the DEAE-Fractogel column. The chromoprotein complex displayed maxima at 416, 483, 542, 622, and 675.5 nm.

D1–D2–Cyt *b*559 samples were placed in EPR quartz tubes (0.3 × 26 cm) at a Chl concentration of 0.15 mg/mL, frozen at liquid nitrogen, and then immediately transferred to the helium cryostat. When the temperature stabilized at 4.5 K, the samples were illuminated with a 150-W projector lamp.

Secondary Electron Transport Activity. Secondary electron transport activity was undertaken at 4 °C using 1 mM $MnCl_2$ and 200 μg/mL silicomolybdate (SiMo) as artificial electron donor and acceptor, respectively. The reduction of SiMo was monitored by the increase in absorption at 600 nm, with a Shimadzu UV-3000 double-beam/dual-wavelength spectrophotometer, shielding the phototube with a Schott BG18 cutoff filter. The D1–D2–Cyt *b*559 complex suspensions were illuminated from the top with a slide projector. The actinic light was filtered through a Schott RG665 cutoff filter and a Schott KG3 heat filter. The intensity of the actinic light at the sample was about 1200 $\mu E/m^2\cdot s$), which was almost saturating for the low level of Chl used. The concentration of reduced SiMo over the period of illumination was calculated using an extinction coefficient of 4.8 $mM^{-1}\cdot cm^{-1}$ (Chapman et al., 1988). Chorophyll content was determined by the method of Arnon (1949).

RESULTS

The electronic absorption spectrum of the D1–D2–Cyt *b*559 complex was measured at 4 °C immediately after elution from the DEAE-Fractogel column. As can be seen in Figure 1, the complex exhibits several bands with maxima at 416, 435, 622, and 675.5 nm due to Chl, at 542 nm due to Pheo (which also contributes to the 416- and 675.5-nm bands), and at 483 nm due to β-carotene. The Soret band of Cyt *b*559 contributes to the 416-nm band.

The effect of TX-100 was monitored following the blue shift of the maximum red band due to the close relationship between the maximum of this band and the electron transport activity of the complex (Seibert et al., 1988; Braun et al., 1990; Booth et al., 1991). Figure 2a shows the evolution of the band maximum during the incubation with 0.05% TX-100. The maxima of the spectra were 675.5 (0 h), 673 (12 h), 672 (20 h), and 671.5 (24 h) nm. A small decrease of band intensity was also observed throughout the incubation

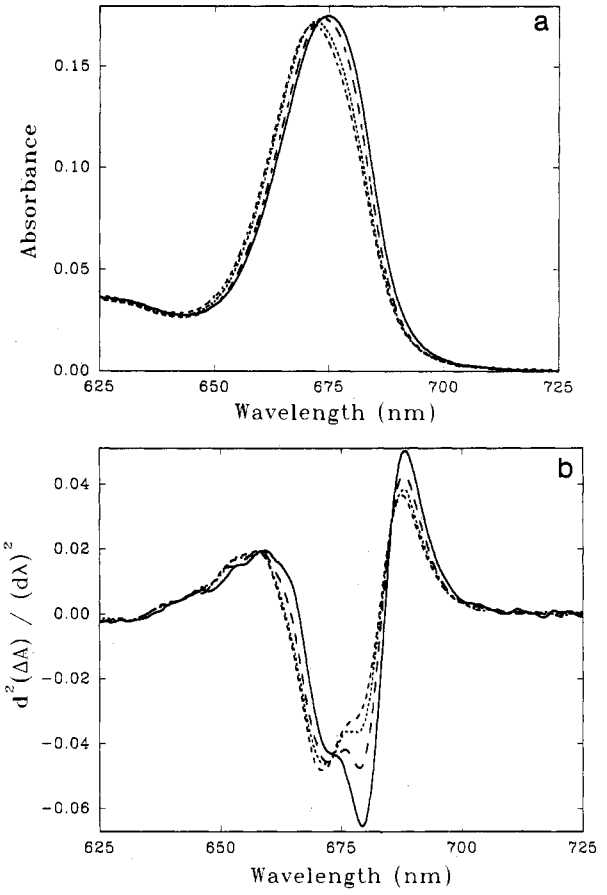

FIGURE 2: (a) Main absorption band in the red region of the D1–D2–Cyt *b*559 complex in a 1-cm path length cuvette measured at successive times during incubation in 50 mM Tris-HCl, pH 7.2, with 0.05% TX-100, at 4 °C in the dark. Solid line, immediately after elution from the column (maximum at 675.5 nm); dashed line, after 16-h incubation (maximum at 673 nm); dotted line, after 20-h incubation (maximium at 672 nm); short-dashed line, after 24-h incubation (maximum at 671.5 nm). (b) Second derivatives of the absorption spectra, showing the evolution of the two components at 679.5 and 670–671 nm during the incubation.

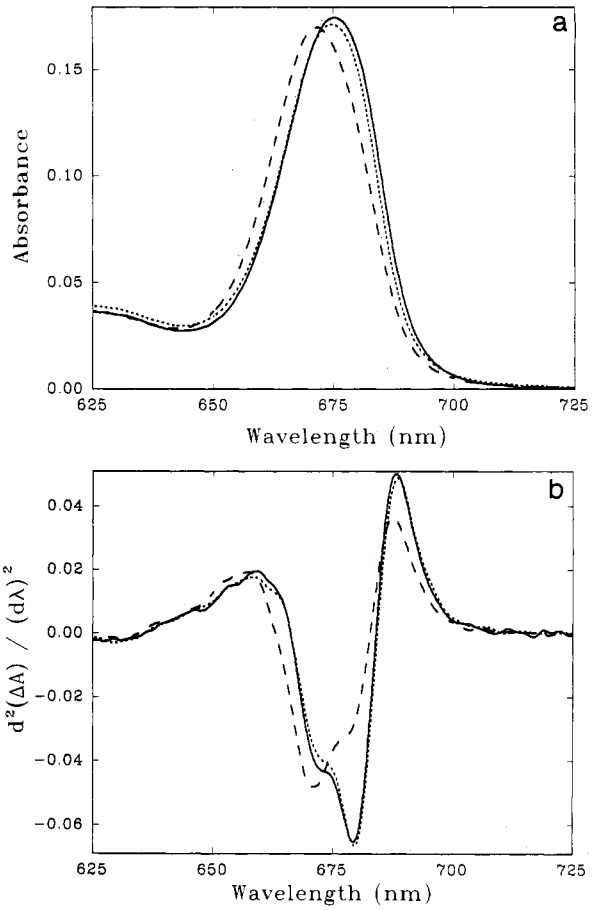

FIGURE 3: (a) Electronic absorption spectra of the native D1–D2–Cyt *b*559 complex (solid line), after 24-h incubation (dashed line), and after detergent exchange (dotted line). (b) Second derivatives of the spectra showing the recovery of the 679.5-nm component after replacement of TX-100 with DM.

time. Second derivatives of the spectra are also plotted in Figure 2b. The second derivative of the native D1–D2–Cyt *b*559 spectrum (maximum at 675.5 nm) showed two components; a main one with a maximum at 679.5 nm and the other represented by a shoulder near 672–673 nm. During the incubation process, the band at 679.5 nm decreased and a component which increased with the incubation time appeared at 670–671 nm. The same behavior was observed using the fourth derivative analysis (not shown).

A sample of partially deactivated D1–D2–Cyt *b*559 complex, which absorbed at 671–671.5 nm, was subjected to detergent exchange (see Materials and Methods) using DM as a new surfactant in the solution. The spectroscopic properties of this sample after detergent exchange were analyzed. Figure 3a displays the spectra of PSII RC complex of the native sample (maximum at 675.5 nm), the deactivated sample (maximum at 671.5 nm), and the reactivated sample (maximum at 675 nm). As shown in this figure, the new spectrum nearly recovered that of the native form. This fact was also demonstrated by the second derivative analysis, which showed a complete recovery of the 680-nm component (Figure 3b), and by the fourth derivative analysis (not shown).

The fluorescence properties of the D1–D2–Cyt *b*559 complex were also studied during the TX-100 incubation process and after detergent exchange. The fluorescence greatly increased with the detergent incubation time. Figure 4 displays the emission spectra of the preparation, obtained immediately after elution from the anion-exchange column, after TX-100 incubation for 24 h, and after detergent exchange. The fluorescence intensity was much higher when the main red absorption band peaked at 670–671.5 nm just before the detergent exchange. This increase in the fluorescence yield was accompanied by a blue shift of the band maximum, i.e., from 682 nm in freshly isolated samples to 672 nm in TX-100-treated samples. Both the fluorescence yield and the band maximum returned to their original values after detergent exchange.

The CD spectrum in the red region of freshly isolated D1–D2–Cyt *b*559 complex showed two components with peaks at 682 nm (+) and 666 nm (–). The changes in the absorption and fluorescence spectral properties during TX-100 incubation and the loss of the 680-nm component were followed by a decrease in the dichroic activity (Figure 5). The CD spectrum of the 671.5-nm-absorbing form depicted a signal 4.5 times smaller than that of the native form. This showed that the chromophores responsible for the optical activity were significantly affected by the TX-100 treatment. On the other hand, after detergent exchange the new CD spectrum was similar to that of the native complex; about 92% of the CD signal was recovered. CD spectroscopy was also carried out in the peptidic bond absorption region (200–250-nm range), looking for conformational changes in the secondary structure of the protein backbone produced by the incubation with TX-100 and after exchanging this detergent with DM. Figure 6 shows the CD spectra in the 200–250-nm range of native

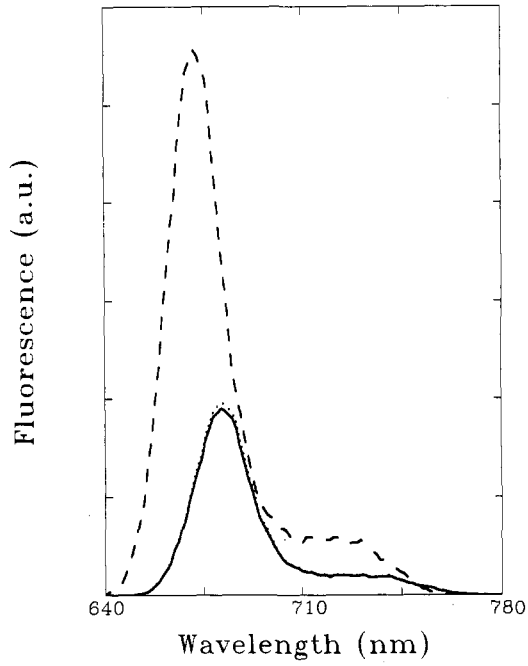

FIGURE 4: Fluorescence spectra of the D1–D2–Cyt *b*559 complex at 4 °C in 50 mM Tris-HCl, pH 7.2, with excitation at 435 nm. Solid line, native D1–D2–Cyt *b*559 complex (measured just after its elution from the column); dashed line, D1–D2–Cyt *b*559 complex preparation after 24-h incubation; dotted line, D1–D2–Cyt *b*559 complex after replacement of TX-100 with DM.

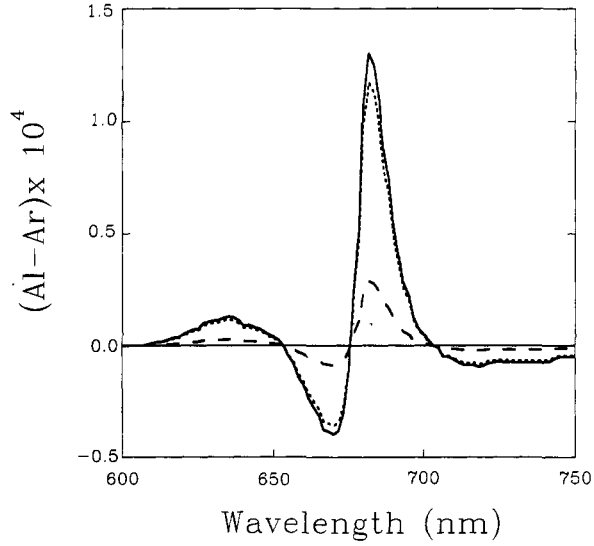

FIGURE 5: Circular dichroism spectra of freshly isolated D1–D2–Cyt *b*559 complex recorded in the red spectral region (600–750 nm) at 4 °C. Solid line, native complex; dashed line, after 24-h incubation in the same buffer with 0.05% TX-100; dotted line, after TX-100 replacement with DM.

D1–D2–Cyt *b*559 complex, TX-100-treated sample, and after detergent replacement. It is apparent that the blue shifts of the absorption and fluorescence bands, the high fluorescence yield, and the reduction of the dichroic activity in the red spectral region coincided with some modifications of the protein secondary structure of the complex. However, the Trp fluorescence, a useful probe for the denaturation of a protein, did not change significantly in TX-100-treated sample compared to that of the native form (Figure 7). This may indicate that the secondary structure was not highly disturbed by TX-100, in agreement with CD data, and/or that no Trp residues are present within the disturbed protein domains. A small reduction of the fluorescence yield and a blue shift from

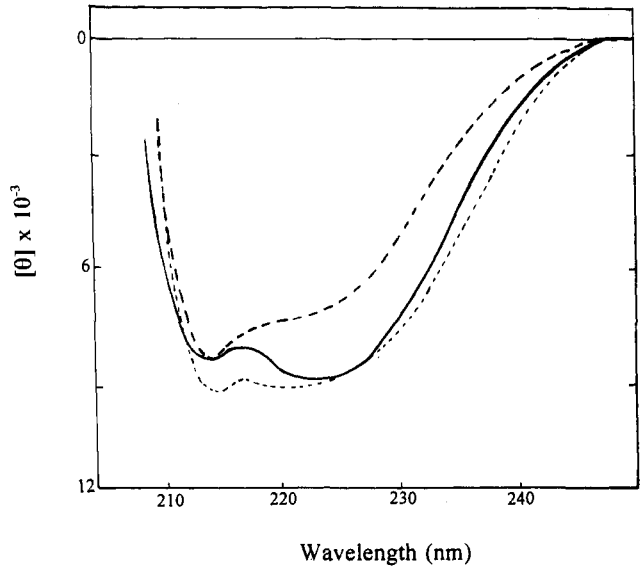

FIGURE 6: Circular dichroism spectra in the peptidic bond absorption region recorded at 4 °C. Solid line, native complex; dashed line, complex after 24-h incubation; short-dashed, complex after substitution of TX-100 with DM. Circular dichroism values are expressed in θ, mean residue weight ellipticity in degrees·centimeter^2·decimole^{-1}.

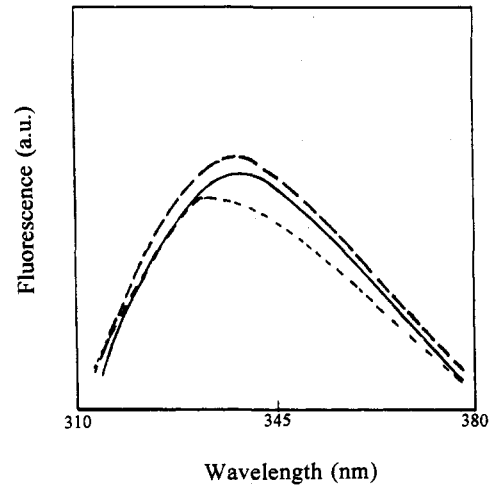

FIGURE 7: Tryptophan fluorescence spectra of the D1–D2–Cyt *b*559 complex at 4 °C under different experimental conditions. Solid line, native complex in 50 mM Tris-HCl, pH 7.2, with 0.05% TX-100 just after elution from the first chromatographic column; dashed line, complex after 24-h incubation; short-dashed line, complex after TX-100 replacement with DM.

339 to 332 nm were observed, however, after detergent exchange, suggesting a more hydrophobic protein environment in the presence of DM.

The characteristic light-induced spin-polarized triplet EPR signal attributed to triplet P680 is considered a reliable probe for the structure/function of PSII RC complex. This spin-polarized triplet EPR signal was detected in our preparation of D1–D2–Cyt *b*559 complex (Figure 8) using the experimental conditions described under Materials and Methods. The shape of the signal was comparable to that reported by other groups using similar D1–D2–Cyt *b*559 preparations (Okamura et al., 1987; Ghanotakis et al., 1989) or less purified PSII samples (Rutherford et al., 1981). The signal in the central part of the spectrum most probably corresponded to Chl^+ species. Due to the high instrument sensitivity used to carry out these experiments, the central-left part of the spectrum was somewhat disturbed by an unknown background signal. For this reason, only the right part of the spectra were used to compare the intensities of the triplet EPR signals

Table 1: Relationship between λ_{max}, Secondary Electron Transport Activity, Dichroic Activity, and Comparative Fluorescence Yield of the D1–D2–Cyt *b*559 Complex

sample[a]	λ_{max} (nm) red band	activity [μequiv of e^- (μmol of Chl)$^{-1}$ h^{-1}]	activity (%)	CD band intensity at 682 nm (%)	CD band intensity at 220 nm (%)	comparative fluorescence yield
native RC	675.5	2640	100	100	100	1
TX-RC	671.5	700	22	20	85	2.88
DM-RC	675	2500	95	92	105	1.031

[a] Native RC, freshly isolated sample; TX-RC, after 24-h incubation in 0.05% TX-100; DM-RC, after TX-100 substitution with DM.

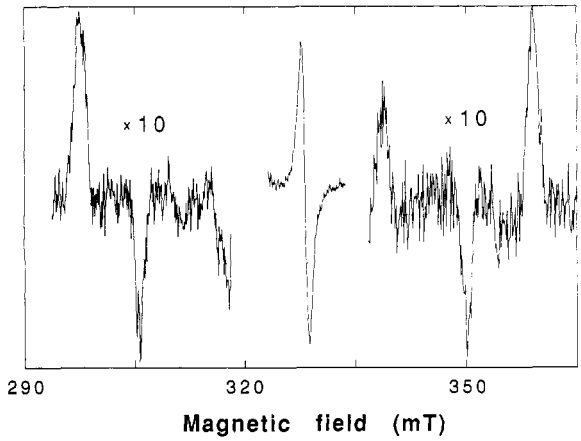

FIGURE 8: Electron paramagnetic resonance spectrum of light-induced triplet in D1–D2–Cyt *b*559 complex. Light source: 150-W projector lamp. Experimental conditions: microwave frequency, 9.26 GHz; modulation amplitude, 10 Gpp (Gauss peak to peak of the EPR spectrum); temperature, 4.5 K; Chl concentration, 0.15 mg/mL.

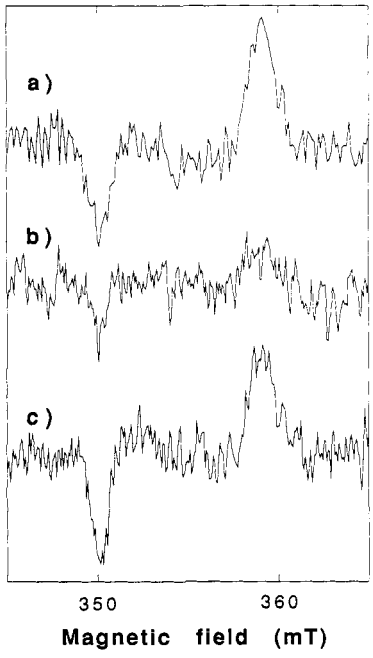

FIGURE 9: Electron paramagnetic resonance spectra of light-induced triplet in native (a), TX-100-treated (b), and renatured (c) D1–D2–Cyt *b*559 complex. The experimental conditions were the same as in Figure 8.

from the three types of samples studied through this work. Figure 9 compares the light-induced triplet EPR signals from native, TX-100-treated, and renatured D1–D2–Cyt *b*559 complex. The intensity of the EPR signal was much smaller in the case of the TX-100-treated sample than that from the control sample. The triplet EPR signal intensity was almost completely recovered after the detergent exchange.

The secondary electron transport was also measured, using $MnCl_2$ and SiMo as artificial electron donor and acceptor, respectively, in native, TX-100-treated, and after detergent exchange samples. The behavior of the secondary electron transfer activity at different TX-100 incubation times (not shown) was very similar to that described by Seibert (1993), consisting of a progressive loss of activity concomitant with a blue shifting of the absorption spectrum during TX-100 treatment. Samples with maxima at 670 nm or lower complete lost their activities. Table 1 compares the band maximum, the secondary electron transport and dichroic activities, and the Chl fluorescence yield for native, partially denatured, and renatured samples.

DISCUSSION

Because of the intrinsic properties of membrane proteins, an important gap exists in our present knowledge of the denaturation and renaturation characteristics of this kind of proteins (Huang et al., 1987; Popot et al., 1987). One common agent used to denature proteins is temperature, but other agents such as urea, polyols, and guanidinium chloride are also effective in destabilizing proteins. In the case of membrane proteins, a common reason for destabilization and loss of activity is the action of detergents, which on the other hand are required for their solubilization and isolation. It is well-known that detergents which are highly effective for the initial dispersion of lipids and membrane fragmentation are not necessarily optimal for keeping the isolated membrane fragments or proteins in their native state in solution. The foregoing principle accounts for the preferred use of detergents with relative high critical micelle concentrations (cmcs) in membrane solubilization (Helenius & Simons, 1975) and suggests, in contrast, that detergents with relatively low cmcs may be superior for keeping a protein in its native state after isolation. This principle seems to hold in the case of the two detergents used in the present study. Indeed, the cmc for TX-100, a "harsh" detergent, is much higher (0.31 mM) than the cmc for DM (0.15 mM), a "milder" detergent. The detergent effect may be the result of a direct binding and interaction with the hydrophobic moiety of membrane proteins.

The damaging effects of TX-100 on the D1–D2–Cyt *b*559 complex described in this paper are in agreement with other studies (Seibert et al., 1988; Tetenkin et al., 1989; Braun et al., 1990; Tang et al., 1991; He et al., 1991). However, our results show that the damage produced in the chromoprotein by this detergent can be reversed under certain conditions. This reversibility was probed by Chl absorption, fluorescence, and CD spectra, the protein secondary structure, and the capability of the RC to catalyze the formation of light-induced spin-polarized triplet EPR signal and secondary electron transport activity.

Due to the spectral congestion in the red region in the D1–D2–Cyt *b*559 complex, the characterization of the different components under the main red absorption band is much more difficult than in the case of the bacterial RC. It is generally accepted that P680 is responsible for a good part of the absorption at 680 nm while the other Chl are responsible for the absorption near 670 nm (van Kan et al., 1990; Braun, et

al., 1990; Montoya et al., 1993; van der Vos et al., 1992; Durrant et al., 1992). The identification of the Pheo molecules is, however, more controversial. Some groups propose that the active Pheo absorbs at 680–681.5 nm (Nanba & Satoh, 1987; Tang et al., 1990; van der Vos et al., 1992), whereas others locate the two Pheo between 670 and 680 nm (van Kan et al., 1990; Braun et al., 1990; Otte et al., 1992; Montoya et al., 1993). Incubation with TX-100 led to a progressive spectral modification; the absorption at 680 nm decreased whereas the 670–nm component increased its importance in the absorption spectrum and in the second derivative (Figure 2). These absorbance changes were more or less conservative, which induced a blue shift of the absorption spectrum. Along with the progressive loss of absorption at 680 nm, the maximum fluorescence band blue-shifted, the fluorescence yield increased, the CD intensity in the red region strongly decreased, and the triplet EPR signal and the secondary electron transport activity diminished. Substitution of DM for TX-100 in damaged D1–D2–Cyt *b*559 complexes (671.5-nm form) resulted in the recovery of the absorption at 680 nm along with all other spectroscopical properties and photochemical activities of the native complex. This strongly suggested that the loss or the recovery of a component absorbing at 680 nm induced all these phenomena.

The light-induced spin-polarized triplet EPR signal described in the Results section is a very characteristic signal attributed to the formation of triplet P680 as a result of charge recombination between $P680^+I^-$. This constitutes a direct probe of both the structure and function of the RC and can also be used as measurement of relative concentration of P680. Thus, the triplet EPR data buttress the spectroscopic and secondary electron transport activity data described in this paper. Indeed, the intensity of the triplet EPR signal closely followed the other parameters described here. It means that the appearance and disappearance of P680 induced all observed changes as a consequence of the rearrangement of pigments.

The reorganization of the pigment–protein complex may explain the fluorescence data. In native D1–D2–Cyt *b*559 complex, where photochemistry takes place, the fluorescence has a maximum at 682–685 nm which comes from the lower energy band at around 680 nm. As P680 becomes unorganized and the photochemistry is impaired by the presence of TX-100, the complex becomes more fluorescent and the maximum shifts to 670–672 nm. This fluorescence comes from monomeric Chl (native 670–nm component and/or that resulted from the disruption of P680), most probably due to a loss of photochemistry. The fluorescence yield of the sample absorbing near 671.5 nm was only 2.88 times higher than that of the native sample (Table 1). Considering the high fluorescence yield of the Chl in solution (Durrant et al., 1990), one would expect a higher fluorescence yield of the TX-100-treated sample if the Chl were detached from the apoprotein moiety. The relatively low fluorescence yield of the TX-100-treated sample compared to native to renatured samples indicates that Chl still remains bound to the apoprotein and does not exist as free Chl. This was also confirmed by the fact that no pigments were detected in the washing buffer during the detergent exchange in the column.

A reorganization of the complex may also explain the decrease of optical activity (CD) induced by incubation with TX-100. The CD doublet in the red spectral region was markedly reduced in the presence of this detergent. These kinds of CD spectra have been ascribed in photosynthetic systems to excitonic interactions between pigment molecules. These interactions are very dependent on the relative orientation and/or distance between the optically active molecules. This means that the chromophores of the D1–D2–Cyt *b*559 complex responsible for the CD signal in the red region were losing their specific orientation and/or distance within the protein matrix during the incubation with TX-100. But it seems that the structure of the CD-active chromophores was almost entirely recovered when DM was substituted for TX-100 (Figure 5). From the data of Table 1 and Figure 9, it is apparent that the CD intensity in the red region correlates to the secondary electron transport activity and the intensity of the triplet EPR signal, and it can be concluded, therefore, that most of the CD signal comes from P680.

The results obtained using CD spectroscopy in the UV region also indicate that pigment–protein reorganization actually takes place within the complex treated with TX-100. The secondary structure of the protein was somewhat modified under these conditions (Figure 6 and Table 1), thus allowing the reversibility of the process. On the other hand, the fact that P680 was highly affected by detergent, without significant disturbance of the Trp fluorescence, suggests that this residue is not present in the P680 domain. Models for the arrangement of D1, D2, and chromophores with respect to the photosynthetic membranes indicate that this is certainly the case (Svensson et al., 1990; Ruffle et al., 1992).

The question arises as to how no major changes in the secondary structure of the protein matrix induce a large effect on P680. The easier but certainly not the only possible explanation is to consider the P680 as a dimer, at least in its ground state. Such a dimer should interact with the protein domain surrounding it. Small modifications of this domain may strongly affect the orientation and/or distance of the two chromophores with respect to each other and to the protein matrix, and thus their interactions. This will result in a disruption of the dimeric structure and then the disappearance of the 680-nm component, which induced all phenomena described through this paper. The structure of P680 domain, which seems to be very sensitive to TX-100, can be reestablished by replacing this detergent with DM.

ACKNOWLEDGMENT

We would like to thank María V. Ramiro for her skillful technical assistance and Drs. M. Becana and J. Sancho for critical reading of the manuscript.

REFERENCES

Arnon, D. I. (1949) *Plant Physiol. 24*, 1–24.
Barber, J., Chapman, D., & Telfer, A. (1987) *FEBS Lett. 220*, 67–73.
Berthold, D. A., Babcock, G. T., & Yocum, C. F. (1981) *FEBS Lett. 134*, 231–234.
Booth, P. J.; Crystall, B., Ahamad, I., Barber, J., Porter, G., & Klug, D. R. (1991) *Biochemistry 30*, 7573–7586.
Braun, P., Greenberg, B. M., & Scherz, A. (1990) *Biochemistry 29*, 10376–10387.
Budil, D. E., Gast, P., Chang, C. H., Schieffer, M., & Norris, J. (1987) *Annu. Rev. Phys. Chem. 38*, 561–583.
Chapman, D., Gounaris, K., & Barber, J. (1988) *Biochim. Biophys. Acta 933*, 423–431.
Dekker, J. P., Bowlby, N. R., & Yocum, C. F. (1989) *FEBS Lett. 258*, 150–155.
Diner, B. A., Petrouleas, V., & Wendoloski, J. J. (1991) *Physiol. Plant. 81*, 423–436.
Durrant, J. R., Giorgi, L. B., Barber, J., Klug, D. R., & Porter, G. (1990) *Biochim. Biophys. Acta 1017*, 167–175.
Durrant, J. R., Hastings, G., Joseph, D. M., Barber, J., Porter, G., & Klug, D. (1992) *Proc. Natl. Acad. Sci. U.S.A. 89*, 11632–11636.

Ghanotakis, D. F., de Paula, J. C., Demetriou, D. M., Bowlby, N. R., Petersen, J., Babcock, G. T., & Yocum, C. F. (1989) *Biochim. Biophys. Acta 974*, 44–53.

Gounaris, K., Chapman, D., Booth, P. J., Crystall, P., Giorgi, L. B., Klug, D. R., Porter, G., & Barber, J. (1990) *FEBS Lett. 265*, 88–92.

He, W. Z., Newell, W. R., Harris, P. I., Chapman, D., & Barber, J. (1990) *Biochemistry 30*, 4552–4559.

Helenius, A., & Simons, K. (1975) *Biochim. Biophys. Acta 415*, 29–79.

Huang, K. S., Bayley, H., Liao, M. J., London, E., & Khorana, G. (1981) *J. Biol. Chem. 256*, 3802–3809.

Ikeuchi, M., & Inoue, Y. (1988) *FEBS Lett. 241*, 99–104.

Kirmaier, C., & Holten, D. (1987) *Photosynth. Res. 13*, 225–260.

Kobayashi, M., Maeda, H., Watanabe, T., Nakane, H., & Satoh, K. (1990) *FEBS Lett. 260*, 138–140.

McTavish, H., Picorel, R., & Seibert, M. (1989) *Plant Physiol. 89*, 452–456.

Michel, H., & Deisenhofer, R. (1988) *Biochemistry 27*, 1–7.

Moënne-Loccoz, P., Robert, B., & Lutz, M. (1989) *Biochemistry 28*, 3641–3645.

Montoya, G., Yruela, I., & Picorel, R. (1991) *FEBS Lett. 283*, 255–258.

Montoya, G., Cases, R., Yruela, I., & Picorel, R. (1993) *Photochem. Photobiol. 58*, 724–729.

Nanba, O., & Satoh, K. (1987) *Proc. Natl. Acad. Sci. U.S.A. 84*, 109–112.

Okamura, M. Y., Satoh, K., Isaacson, R. A., & Feher, G. (1987) in *Progress in Photosynthesis Research* (Biggens, J., Ed.) Vol. 1, pp I.4.379–381, Martinus Nijhoff Publishers, Dordrecht, The Netherlands.

Otte, S. C. M., van der Vos, R., & van Gorkom, H. J. (1992) *J. Photochem. Photobiol. 15*, 5–14.

Popot, J. L., Gerchman, S. E., & Engelman, D. M. (1987) *J. Mol. Biol. 198*, 655–676.

Ruffle, S. V., Donnelly, D., Blundell, T. L., & Nugent, J. H. A. (1992) *Photosynth. Res. 34*, 287–300.

Rutherford, A. W., Paterson, D. R., & Mullet, J. E. (1981) *Biochim. Biophys. Acta 635*, 205–214.

Seibert, M. (1993) in *The Photosynthetic Reaction Center* (Deisenhofer, J., & Norris, J., Eds.) Vol. 1, pp 319–356, Academic Press, Orlando, FL.

Seibert, M., Picorel, R., Rubin, A., & Connolly, J. S. (1988) *Plant Physiol. 87*, 303–306.

Svensson, B., Vass, I., Cedregren, E., & Styring, S. (1990) *EMBO J. 9*, 2051–2059.

Tang, D., Jankowiak, R., Seibert, M., & Small, G. J. (1990) *J. Phys. Chem. 94*, 6519–6522.

Tang, D., Jankowiak, R., Seibert, M., & Small, G. J. (1991) *Photosynth. Res. 27*, 19–29.

Tetenkin, V. L., Gulayev, B. A., Seibert M., & Rubin, A. B. (1989) *FEBS Lett. 250*, 459–463.

Trebst, A. (1986) *Z. Naturforsch. 41c*, 240–245.

van der Vos, R., van Leeuwen, P., Braun, B. M., & Hoff, A. J. (1992) *Biochim. Biophys. Acta 1140*, 184–198.

van Kan, P. J. M., Otte, S. M. C., Kleherenbriak, F. S. M., Nieveen, M. C., Aartsma, T. J., & van Gorkom, H. J. (1990) *Biochim. Biophys. Acta 1020*, 146–152.

van Mieghem, F. J. E., Satoh, K., & Rutherford, A. W. (1991) *Biochim. Biophys. Acta 1058*, 379–385.

Youvan, D. C., Bylina, E. J., Alberti, M., Begush, H., & Hearst, J. E. (1984) *Cell 37*, 949–957.